

## RECENT DEVELOPMENTS IN THE CONTAIN-LMR CODE\*

K. K. Murata  
Sandia National Laboratories  
Albuquerque, New Mexico 87185

SAND--89-3029C  
DE90 012184

## ABSTRACT

Through an international collaborative effort, a special version of the CONTAIN code is being developed for integrated, mechanistic analysis of the conditions in liquid metal reactor (LMR) containments during severe accidents. The capabilities of the most recent code version, CONTAIN LMR/1B-Mod.1, are discussed. These include new models for the treatment of two condensables, sodium condensation on aerosols, chemical reactions, hygroscopic aerosols, and concrete outgassing. This code version also incorporates all of the previously released LMR model enhancements. The results of an integral demonstration calculation of a severe core-melt accident scenario are given to illustrate the features of this code version.

## INTRODUCTION

A special version of the CONTAIN code<sup>1</sup> is currently being developed to analyze the thermal-hydraulic and radiological conditions within the containment of a liquid-metal reactor (LMR) during a severe accident. The CONTAIN code has been under development for many years as the U. S. Nuclear Regulatory Commission's (USNRC's) best-estimate containment analysis code. The models in the code developed under USNRC funding encompass atmosphere thermal-hydraulics, radiative and convective heat transfer to structures, aerosol and fission product transport, fission product decay heating, hydrogen burns, and core-concrete interactions. The USNRC code versions, referred to as base versions below, are also capable of treating sodium as the coolant and in addition have models for sodium atmosphere chemistry and sodium spray and pool fires. USNRC funding of the liquid metal reactor aspects of the code ended with the demise of the Clinch River Breeder Reactor Project. However, since that time, members of the CONTAIN LMR user's group in the U. S., Japan, and Germany have become involved in a collaborative effort with Sandia National Laboratories to develop and verify the LMR aspects of the code further, and a number of LMR enhancements to the base versions have been developed as a result of this collaboration.

---

\*This work supported by the United States Nuclear Regulatory Commission under FIN #A1849 and by contracts with PNC, Japan; the Gesellschaft fuer Reactorsicherheit, FRG; and Westinghouse Hanford. This work has been performed at Sandia National Laboratories, which is operated for the U. S. Department of Energy under contract number DE-AC04-76DP00789.

## **DISCLAIMER**

**This report was prepared as an account of work sponsored by an agency of the United States Government. Neither the United States Government nor any agency Thereof, nor any of their employees, makes any warranty, express or implied, or assumes any legal liability or responsibility for the accuracy, completeness, or usefulness of any information, apparatus, product, or process disclosed, or represents that its use would not infringe privately owned rights. Reference herein to any specific commercial product, process, or service by trade name, trademark, manufacturer, or otherwise does not necessarily constitute or imply its endorsement, recommendation, or favoring by the United States Government or any agency thereof. The views and opinions of authors expressed herein do not necessarily state or reflect those of the United States Government or any agency thereof.**

## **DISCLAIMER**

**Portions of this document may be illegible in electronic image products. Images are produced from the best available original document.**

For completeness, the features of previously released base and LMR code versions will first be reviewed. The first code with LMR enhancements to be officially released, CONTAIN LMR/1A,<sup>2</sup> is based on the CONTAIN 1.06 base version. The principal LMR enhancements in the LMR/1A code include the SLAM sodium-concrete interaction code, developed at Sandia<sup>3</sup> and implemented into CONTAIN as a joint effort between Sandia and PNC, Japan, and the CONTAIN debris bed model. The latter model describes the coolability of ex-vessel debris beds, their quenching by sodium, and the transition to the start of core-concrete interactions.<sup>2</sup>

More recent LMR enhancements and generic improvements are also discussed below. Many of the more recent LMR enhancements, along with the previously released ones, have been adapted to the CONTAIN 1.11 base version to produce the LMR code version, CONTAIN LMR/1B-Mod.1, that is the focus of this paper. This LMR code version includes all of the models discussed in this paper, unless otherwise noted. The 1.11 base version itself offers a number of substantially improved or new generic models. The major new models in the 1.11 base version of interest here include a hygroscopic aerosol model and a quasi-mechanistic concrete outgassing model, developed originally as an LMR enhancement. The hygroscopic aerosol model is a generalization of the MAEROS-based aerosol module in CONTAIN to include solubility and surface tension effects in the modeling of condensation of water on aerosol particles.<sup>4</sup> The quasi-mechanistic outgassing model<sup>5</sup> offers significant advantages in computational efficiency over the outgassing option based on the SLAM model. The more recent LMR-specific enhancements available in the LMR/1B-Mod.1 code include the ability to treat sodium and water simultaneously as condensable materials within the same problem, the modeling of sodium condensation on aerosols, and an extensively revised sodium chemistry package.

An integral LMR demonstration calculation using an interim version of the LMR/1B-Mod.1 code is presented to illustrate the operational status of a large number of models of interest to LMR analysis. The calculation describes a relatively severe core-melt accident scenario which leads to containment venting after a relatively short period (20 hours). This scenario is of particular interest because it shows that the new code features are important for the proper calculation of aerosol deposition rates in the problem. These rates are sufficient to reduce the amount of particulate fission products vented from the containment by many orders of magnitude.

#### LMR MODELING AND CODE DEVELOPMENT

This section discusses the models presently available for LMR modeling. With a few exceptions, the models are presented in one of the three subsections below according to whether a model was first available in a released base version, the LMR/1A code, or the LMR/1B code. However, unless otherwise noted, they are all available in the LMR/1B-Mod.1 code.

##### The Base Versions

The base versions offer a broad variety of models in a system-level computational structure, which allows for complex interactions and

feedback among the models. In the most recently released base version, CONTAIN 1.10,<sup>1</sup> there are models for:

- Intercell gas flow, with a fully non-linear, pressure-implicit solution algorithm.
- Buoyancy-driven natural convection circulation between cells.
- Single-condensable, two-phase thermodynamics.
- Convective, condensation and radiative heat transfer between the atmosphere and heat transfer structures or between the atmosphere and the reactor cavity model.
- Hydrogen combustion.
- Basic aerosol processes including condensation, agglomeration, and deposition, calculated according to a discrete size-class representation of particle sizes.
- Transport and decay of fission products and their decay heating.
- Reactor cavity models, including a thermal-conduction model, a pool boiling model, and a core-concrete interaction model.
- LWR-oriented engineered systems models.
- Pool scrubbing and vapor evolution associated with gases vented into pools of coolant.
- Sodium atmosphere chemistry
- Sodium pool and spray fires

Space limitations do not permit a general discussion of the above models to be given here. However, the core-concrete interaction model and the sodium-specific models are discussed in the context of the LMR code in the following sections. The interested reader should consult Reference 1 for details on the other models.

#### Models in CONTAIN LMR/1A

Because of the importance of the interactions in the reactor cavity in determining the consequences of an extended accident scenario, the most extensive of the LMR enhancements model various types of interactions in the reactor cavity. As discussed below, three types of interactions are explicitly modeled in CONTAIN LMR/1A: sodium-debris-bed interactions, core-concrete interactions, and sodium-concrete interactions.

Sodium-Debris-Bed Interactions. Recently, Sandia has developed a debris bed model for the LMR code.<sup>2</sup> This model, while relatively simple, treats both coolable and uncoolable beds. Detailed mechanistic description of the process of the formation of the debris bed or of its subsequent quenching is not the goal of this model. Rather, it is to determine the outcome of a major branch point in the evolution of an accident scenario, which depends on the coolability of the bed. The model uses bed parameters specified by the user to determine bed coolability. If the bed is coolable and sufficient coolant is present, then the onset of core-concrete interactions may be delayed significantly, and the outcome of the scenario may be significantly altered by that delay. If the bed is coolable, a simple approach is used to calculate the rate of quenching of the bed and the heating of the pool. A variety of criteria may be specified by the user with respect to the remelt of the bed. Upon

remelt, a transition is made to the CORCON core-concrete interaction model.

Core-Concrete Interactions. As in the base versions, the interactions of molten core debris with concrete, following primary vessel melt-through, are modeled through integrated versions of the CORCON-MOD2 code<sup>6</sup> and the VANESA code.<sup>7</sup> CORCON models the thermal attack of core debris on the concrete surface of the reactor cavity, using a two-dimensional axisymmetric model of the melt and the ablating concrete. The ablated concrete is incorporated into the melt and the gases evolved from the concrete are allowed to react with the metallic species in the melt. In the LMR code, the gases evolving from the top surface of the core debris are allowed to react further with the sodium in an overlying pool, if one exists. For LWR applications, VANESA models the release of aerosols and fission products due to the gases sparging, or bubbling, through the core debris.<sup>7</sup> If an overlying coolant pool is present, the scrubbing of these gases with respect to aerosols and fission products is also modeled.

For LWRs, CORCON and VANESA constitute a package suitable for describing the long-term interactions and sources arising in the cavity from melted core debris. However, in its present form, the VANESA modeling of aerosol and fission product generation omits processes important for LMRs. This modeling assumes that aerosol and fission product generation occurs only as the result of gas sparging. For LMRs a more general model is needed to take into account the affinity of the sodium pool for fission products and the vaporization release of fission products directly from the sodium pool. The development of such a model has begun at Sandia.

Sodium-Concrete Interactions. Sodium-concrete interactions result from the chemical attack of the concrete by sodium, accompanied by the outgassing of bound and evaporable water and bound CO<sub>2</sub> from the concrete and ablation of the concrete surface. These interactions are modeled in CONTAIN through an integrated version of the SLAM code, which has been developed and verified at Sandia.<sup>3</sup> This model uses a one-dimensional, three-region formulation which takes into account the wet (hydrated) region of the concrete, the dehydrated region, and the boundary layer between the pool and the concrete. One-dimensional mass, momentum, and energy equations are solved in each region, along with chemical kinetics equations. An option to calculate simple outgassing of the concrete with the SLAM model in the absence of sodium chemical reactions is being developed.

#### Models in CONTAIN LMR/1B

Besides the models discussed above, a number of new containment atmosphere models are available in the LMR/1B-Mod.1 code. Two of these models, the hygroscopic aerosol model<sup>4</sup> and the quasi-mechanistic outgassing model,<sup>5</sup> are also available in the CONTAIN 1.11 base version.

Two-Condensable Modeling. In the base versions, all gases except the coolant vapor are treated as noncondensables. However, calculations such

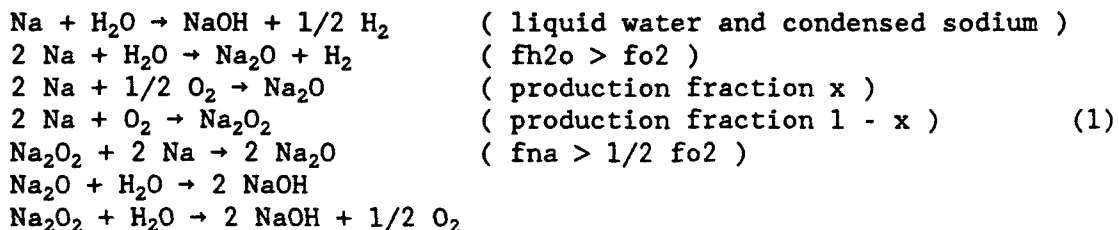
as the integral demonstration calculation presented below show that it is desirable that both sodium and water be treated as condensables within the same problem.

The treatment of the two condensables is different for processes occurring entirely within the atmosphere and for those occurring at interfaces between the atmosphere and structures or pools. For the former, the treatment is a general one. For example, within the atmosphere thermodynamics and intercell flow module, sodium and water are treated on the same footing as potentially two-phase materials in each CONTAIN control volume, or cell.

For simplicity, in treating certain interface processes, only one condensable in each cell (sodium or water, as specified by the user) is considered. These processes include condensation on or evaporation from a pool or a liquid film on the surface of a heat transfer structure. Because of the relatively low temperatures at which these processes are important for water, compared to those for sodium, it is assumed that the cells in which these interface processes are important for water are distinct from those in which the corresponding processes are important for sodium. While it is true that both water and sodium will tend to condense out in a cell that is sufficiently cold, it is likely from the standpoint of the kinetics that sodium vapor introduced into a cold cell will either react or condense rapidly on aerosols and that its condensation on pools or structures will be relatively unimportant.

Sodium Condensation on Aerosols. In recent work by PNC, the CONTAIN aerosol model was modified to treat the condensation of sodium vapor; prior to this effort, only the condensation of water on aerosols had been modeled. In the LMR/1B-Mod.1 code, the PNC modeling has been generalized to allow either sodium or water to condense on aerosols as thermodynamic conditions dictate.

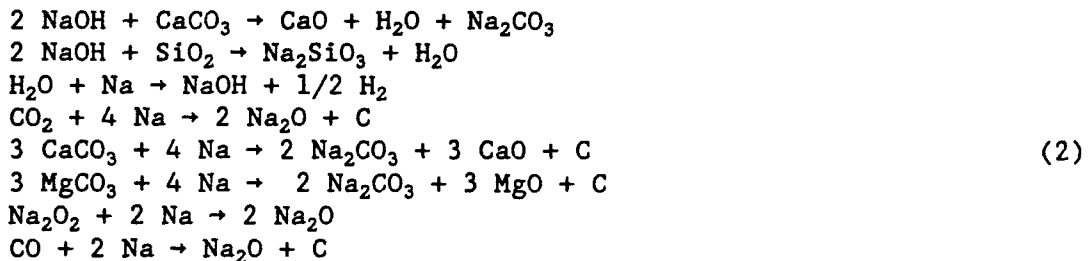
A Revised Atmosphere Chemistry Model. The new two-condensable and aerosol condensation modeling requires an extensive generalization of the atmosphere chemistry model because of the new repositories in which sodium and water reactants can reside. The repositories include the atmosphere gas, aerosols, surface condensate films, and aerosol deposits. The atmosphere chemistry model has been generalized to include the new repositories and the presence of condensed phases of water and sodium. In addition, the chemical species considered have been generalized to include  $\text{Na}_2\text{O}_2$ . (The production of  $\text{Na}_2\text{O}_2$  is modeled in the sodium spray fire and the sodium pool fire models but was not modeled in the burning of sodium vapor. Also, its subsequent reactions were not modeled.) The revised reaction hierarchy as follows:



where  $fh_{20}$ ,  $fo_2$ , and  $fna$  are the gas molar fractions of water vapor, oxygen, and sodium vapor, respectively, and  $x$  is the user-specified molar fraction for the production of the monoxide in atmosphere reactions. The second and fifth reactions are not allowed for  $H_2O$  vapor or Na vapor, respectively, if the indicated conditions on the gas molar fractions are not satisfied. Otherwise, the above reactions are assumed to go to completion instantaneously in the order given. Within a given cell, gas phase reactants are assumed to react with aerosol reactants and with surface reactants. In cases in which a given reactant is completely depleted, reactions within a given repository are considered to occur first, gas-aerosol reactions second, and gas-surface reactions last. Note that aerosol-aerosol reactions are allowed. For example, sodium and water may both be present on aerosol particles, and the amounts present on the same particle are assumed to react. Since the reactions on the same particle are assumed to be instantaneous, the reaction rate is in effect controlled by aerosol processes, such as the agglomeration rate of sodium-bearing and water-bearing aerosols.

The revised atmosphere chemistry model does not modify the way CONTAIN treats the special cases of sodium spray fires or sodium pool fires. Because of the significant potential threat to containment from these processes and the importance of reaction rates for these processes in determining containment loads, the reaction rates for these processes are explicitly modeled. The model for sodium pool fires is taken from the SOFIRE-II code,<sup>8</sup> and that for spray fires from the NACOM code.<sup>9</sup> Because of significant improvements to these models developed at KfK, West Germany, and PNC, it is anticipated that these models will be revised in the near future.

A Revised Pool Chemistry Model. The pool chemistry model, which deals with the reactions of materials contained within a sodium pool, has been brought to operational status in LMR/1B-Mod.1 code. The reactions may involve aerosols which have settled into the pool, gases and concrete ablation products generated in sodium-concrete and core-concrete interactions, and reaction products from pool fires. In addition, the reaction hierarchy has been generalized to be consistent with CO production from CORCON and the possible presence of  $Na_2O_2$ :



These reactions are assumed to go to completion in the order given, and thus the only gases that will escape from the upper surface of a sodium pool are hydrogen and sodium vapor. Consequently, the atmosphere chemistry model does not presently address the presence of CO and  $CO_2$ .

Hygroscopic Aerosol Model. The condensation algorithm in the MAEROS-based aerosol model in CONTAIN has recently been generalized to include the effects of solubility and surface tension.<sup>4</sup> The solubility effect is the effect of principal interest here and refers to the enhanced condensation of water on a particle containing soluble material, because of the decrease in equilibrium vapor pressure above a solution. The sodium aerosols generated in an LMR accident scenario will first react with water, but once the stable hydroxide has formed, the resulting aerosols will also be highly soluble or hygroscopic.

The LWR-oriented LACE experiments examined, among other things, the importance of solubility effects.<sup>10</sup> As expected, the experiments show that condensation of steam on aerosols and the subsequent rain-out can be an extremely effective deposition mechanism for removing particulates from the atmosphere. Moreover, one can infer from these experiments that the solubility of the particulates involved is an important factor in determining the rate of deposition for atmospheres close to saturation.

Concrete Outgassing. Because of the relatively high temperatures expected in an LMR containment during a severe accident and the long duration of many of the accident scenarios, significant outgassing of bound and evaporable water may occur from concrete exposed to elevated temperatures. This water may be important in chemical reactions, especially in inerted parts of the containment. If this water is vented away from the sodium-filled compartments to cooler parts of the containment and condenses on the highly hygroscopic aerosols likely to be present, the deposition of these aerosols and the particulate fission products attached to them may be greatly enhanced. An example of this enhancement is shown below in the integral demonstration calculation.

Recently Sandia completed the development of a computationally efficient, quasi-mechanistic model for concrete outgassing, which is suitable for use with the large number of concrete structures typically present in a containment problem.<sup>5</sup> This model has been installed in CONTAIN 1.11. For the LMR code, the model present in CONTAIN 1.11 has been extended to redirect the evolved gases to a user-specified cell.

#### AN INTEGRAL LMR DEMONSTRATION CALCULATION

An integral LMR demonstration calculation (ILMRDC) has been carried out with an interim version of the LMR/1B-Mod.1 code to demonstrate the operational status of many of the model enhancements discussed above. The scenario chosen for this calculation is a severe core-melt accident scenario with sodium-concrete and core-concrete interactions in the reactor cavity.

##### The Accident Scenario

The ILMRDC describes an accident scenario initiated by a hypothetical core disruptive accident (HCDA) at time zero, followed by head failure and release of fuel, sodium, and fission products to the inner containment. Vessel melt-through is assumed to follow at 3000 seconds, and 60 tons of

core debris and 365 tons of sodium in the primary system are transferred to the reactor cavity.

The ILMRDC uses the same basic LMR plant configuration and fission product source term to containment as an earlier LMR demonstration calculation, referred to below as the LMRDC.<sup>11</sup> As discussed below, the LMRDC exercised many of the basic models in CONTAIN but not the more recent LMR enhancements. The plant configuration is shown in Figure 1 and consists of an inerted (0.9% O<sub>2</sub>) steel-lined inner containment, modeled with cells 1-4, and an outer containment, modeled with cells 5-6. Controlled venting of the containment occurs from the inner containment to the outer containment and then to the environment through filters, if necessary. (Uncontrolled venting from a failed containment is also possible, although on the basis of the postulated containment specifications, higher pressures than those calculated here would be required for failure to occur.)

The present ILMRDC differs from the LMRDC in a number of ways that tend to increase containment loads. First of all, the thermal-hydraulic conditions in the inner containment are not mitigated by active cooling systems in the reactor cavity as in the LMRDC, since these are assumed not to be part of the containment design. Second, substantial barriers to prevent core-concrete and sodium-concrete interactions in the cavity are assumed to be absent. Third, the decay power associated with the core debris in the reactor cavity corresponds to a 1400 Mwt core, which is larger by a factor of approximately two than that assumed in the LMRDC. Finally, the steam outgassed from the concrete behind the steel liner in the inner containment is assumed to be vented directly into cell 6 of the outer containment and not to condense out in the condensation unit of a heat exchanger.

Two mitigation systems assumed operational in the LMRDC are assumed to be operational in the present calculation. The first is a passive system of vents for cooling the reactor cavity atmosphere through natural convection. As shown in Figure 1, a circulation loop involving the four cells of the inner containment is created by these vents. In addition, active heat exchangers for cooling the outer containment atmosphere are assumed to be present, with the same characteristics as in the LMRDC.

For possible comparison purposes, the sodium oxide aerosol, fuel aerosol, and fission product sources to the inner containment are taken to be the same in the ILMRDC and the LMRDC. However, six aerosol components (Na<sub>2</sub>O<sub>2</sub>, Na<sub>2</sub>O, NaOH, UO<sub>2</sub>, Na, and H<sub>2</sub>O) are used in the ILMRDC to track the effects of chemistry and of sodium and water condensation in the inner and outer containments, respectively. As in the LMRDC, ten aerosol size classes and 61 radionuclides from the seven fission product release groups listed in Table I are tracked.

In the presence of rapid aerosol deposition in containment, the late time release of fission products from containment may depend to a large extent on the intermediate and late-time releases of fission products within containment, even if these releases are relatively small. Thus, in the present calculation, as in the LMRDC, extended fission product

vaporization sources, principally from the sodium pool, are considered. Nominal pool vaporization release rates are assigned to each of the seven fission product release groups as indicated in Table I.

Code features exercised in the present calculation but not in the LMRDC include:

- Treatment of two condensables. Two-phase mixtures of sodium and water are modeled in the atmosphere thermodynamics and intercell flow calculations. Water condensation on surfaces is assumed to occur in the outer containment (cells 5-6), while sodium condensation on surfaces is assumed to occur in the inner containment (cells 1-4).
- Sodium and water condensation on aerosols. Although atmospheres saturated with sodium were present in the LMRDC, indicating that sodium condensation on aerosols would occur, sodium aerosol condensation was not modeled in the LMRDC.<sup>11</sup> Also, water could not be treated as a second condensable in the code version used. In the present calculation the enhancement of water condensation on aerosols due to the hygroscopic nature of sodium aerosols is explored in one run via the new hygroscopic aerosol model.
- Revised atmosphere chemistry. The revised atmosphere chemistry model described above is used to calculate the burning of sodium vapor and aerosols vented from the inner to outer containment. These reactions are assumed to produce  $\text{Na}_2\text{O}_2$ ,  $\text{Na}_2\text{O}$ , and  $\text{NaOH}$  according to Equation (1).
- Revised pool chemistry. The revised pool chemistry model described above is used.
- Concrete outgassing. The quasi-mechanistic outgassing model is used for the inner containment and the water outgassed from the concrete in the inner containment is directed to cell 6.
- Sodium-debris-bed interactions. A debris bed is assumed to form in the reactor cavity just after vessel melt-through. Although the debris bed model is invoked, the debris is assumed not to be coolable, and core-concrete interactions are initiated 200 seconds after melt-through.
- Core-concrete interactions. The CORCON core-concrete interaction model is invoked from 200 seconds after vessel melt-through until the end of the calculation. However, the VANESA aerosol and fission product release model is not used. As discussed above, the fission products in the sodium pool are assigned the pool release rates given in Table I.
- Sodium-concrete interactions. The SLAM model is used to calculate the effects of sodium-concrete interactions. These are assumed to initiate at vessel melt-through, due to liner failure from the hot core debris, and occur over an effective area of roughly one third of the cavity floor area. Due to the computational expense of the SLAM

model and the expectation that the interaction is self-limiting from the build-up of reaction products, sodium-concrete interactions are terminated after 1000 seconds.

- Radiative heat transfer. Radiative heat transfer is treated in the reactor cavity. Infrared-active gases in the inner containment will react rapidly with sodium, and thus the radiative transfer in the atmosphere will be controlled primarily by sodium aerosols with a relatively high scattering albedo. Unfortunately, the CONTAIN gas emissivity model assumes that any aerosols present are purely absorbing. Thus it is not used, and instead the radiative transfer is modeled in terms of a direct exchange between the pool and other structure surfaces in the reactor cavity, with a nominal effective emissivity of 0.2 for all surfaces.

#### Results of the Calculation

Figure 2 shows the gas pressures calculated in the ILMRDC for cells 4-6. The differences in the pressures of cells 1-4, which arise from buoyancy effects, are not resolvable on the plot. However, they are sufficient to produce strong natural circulation in cells 1-4 throughout the calculation, except for a short period after vessel melt-through, the starting point of the calculation. The increase in pressure in cell 4 beginning at 3.6 hours marks the end of the period in which relatively cold liquid sodium from the pressure vessel is added to the reactor cavity. Because of the heating and evolution of gases in the inner containment, the flows from the inner containment to the outer containment continue through the end of the calculation at 33 hours. This flow occurs primarily through leakage paths between the inner and outer containment. However, just after vessel melt-through and between 6 and 9 hours the pressure difference is sufficient to open the relief valve between cells 4 and 6. At 20 hours, the pressure build-up in cell 6 causes venting from the outer containment to the environment, and by careful inspection of the figure one can see that the build-up of pressure stops at this point. By contrast, venting in the LMRDC was delayed until 10 days.

The calculated atmosphere temperatures for cells 1-4 and 6 are shown in Figure 3. (The behavior of the temperature in cell 5 is similar to that in cell 6.) The sudden increase in the temperature in cell 1 beginning at 3.6 hours marks the end of the period in which relatively cold sodium from the vessel is added to the reactor cavity. The natural convection in the inner containment increases as a result of this increase in temperature.

The airborne amounts of three selected radionuclides,  $Xe^{133}$ ,  $Cs^{137}$ , and  $Pu^{239}$ , are given in Figures 4-6 for different cells. In Figure 4, the amounts of  $Xe^{133}$  in various cells are given to illustrate the behavior of a radionuclide that is not subject to significant deposition. One should note that the total amount of  $Xe^{133}$  is not constant but is slowly increasing with time during the calculation. This is due to the decay of significant amounts of  $I^{133}$  in the pool to  $Xe^{133}$ . Although the  $I^{133}$  itself is not extremely volatile, any  $Xe^{133}$  formed from its decay is assumed to be immediately released from the pool to the atmosphere. The sudden

increase in  $Xe^{133}$  in cell 6 beginning at 6 hours is due to the opening of the pressure relief valve between cells 4 and 6.

$Cs^{137}$  is chosen as an example of a radionuclide from the most volatile (non-noble-gas) pool release group (Group 3 in Table I), and  $Pu^{239}$  is chosen as an example of the least volatile (Group 7). Once airborne, the  $Cs^{137}$  and  $Pu^{239}$  are assumed to condense completely and be carried by the sodium aerosol components and the  $UO_2$  aerosol component, respectively, of the suspended aerosols.

Figure 5 shows the behavior of the airborne  $Cs^{137}$  and  $Pu^{239}$  in cell 4, which is typical of that in the inner containment. The rapid initial decrease of the  $Cs^{137}$  and  $Pu^{239}$  airborne masses is due primarily to sodium condensation on aerosols and subsequent rainout. This rainout is apparently extremely effective in removing particulates from the inner containment atmosphere but was not modeled in the LMRDC.<sup>11</sup> Another potentially important process for the removal of particulate fission products is agglomeration with aerosols produced from sodium reactions, which enhances settling. In the inner containment, the effect of such agglomeration and settling is much less important than condensation. However, this latter process is important in the outer containment when condensation is absent. The structure observed in the curve for  $Cs^{137}$  around 5 hours is the result of the vaporization release of  $Cs^{137}$  in the cavity, coupled with the increased natural convection in the inner containment beginning at 3.6 hours. As shown in this figure, the  $Cs^{137}$  and  $Pu^{239}$  masses in cell 4 reach a quasi-equilibrium value at late time, determined by the balance between deposition and vaporization of fission products from the pool. The enhanced deposition of fission products from sodium condensation on aerosols, which continues to occur at late times, reduces this equilibrium value considerably from what it would otherwise be. Note that  $Cs^{137}$  and  $Pu^{239}$  would behave approximately like the  $Xe^{133}$  in the absence of deposition effects.

Figure 6 gives the suspended masses of  $Cs^{137}$  and  $Pu^{239}$  in cell 6 of the outer containment. The initial rise in the suspended masses in cell 6 is due to venting from the inner to outer containment just after vessel melt-through. The accelerated decrease in the suspended masses beginning around 10 hours is the result of water condensation on aerosols and subsequent rainout; the atmosphere becomes saturated with the water from concrete outgassing at about this time. At earlier times the deposition of particulate fission products is due primarily to agglomeration and settling. The relatively large amount of  $Cs^{137}$  at late times, compared to the  $Pu^{239}$ , is due to much higher pool release rates for  $Cs^{137}$ . Because of much higher deposition rates in the present calculation, at the respective times of venting, the amount of  $Cs^{137}$  suspended in the outer containment in the present calculation is comparable to that found in the LMRDC,<sup>11</sup> even though considerably more flow occurs from the inner to outer containment in the present calculation and the time for deposition is significantly shorter (20 hours as opposed to 10 days). By contrast, at the respective times of venting, much less  $Pu^{239}$  is suspended in the outer containment in the present calculation than in the LMRDC.

If hygroscopic effects are treated, as they were in one run, the effect of condensation becomes even more pronounced. The suspended Cs<sup>137</sup> and Pu<sup>239</sup> masses calculated in this run are given by the curves labeled CS137-HYG and PU239-HYG in Figure 6. It is clear that the early deposition from condensation is enhanced considerably by the hygroscopic effects. Figure 7 shows the suspended water and sodium hydroxide aerosol mass concentrations in cell 6 in the calculation without hygroscopic effects and the suspended water mass concentration in the one with hygroscopic effects. As expected, water is present on aerosols prior to the onset of saturated conditions when hygroscopic effects are taken into account. (One should note that for a given amount of water on aerosols, the deposition rate for water in the hygroscopic case is usually higher than in the non-hygroscopic case. The reason is that the distribution of water on aerosols is skewed toward the larger aerosols containing NaOH in the hygroscopic case and larger aerosols settle faster.) The enhanced deposition from hygroscopic effects may not continue indefinitely. One reason is that with hygroscopic effects, more water condenses out at early times, leaving less water to condense at later times. In Figure 6, the fact that the suspended masses with and without hygroscopic effects attain approximately the same quasi-equilibrium value after 20 hours indicates that the deposition rates have become comparable.

As a result of the filtered venting of cell 6, a calculated cumulative amount of  $1.3 \times 10^{-6}$  kg of Cs<sup>137</sup> and  $1.1 \times 10^{-8}$  kg of Pu<sup>239</sup> is vented into the filter trains up to 33 hours, if no credit is taken for hygroscopic effects. The amount of Pu<sup>239</sup> vented would clearly be reduced substantially with hygroscopic effects.

#### CONCLUSIONS

The capabilities of the CONTAIN code for LMR analysis have been reviewed, and the features of the most recent LMR code version, CONTAIN LMR/1B-Mod.1, have been discussed. This code version includes most of the recent LMR model enhancements and important new CONTAIN generic models, as well as the previously released LMR enhancements. An integral demonstration calculation of a relatively severe core-melt accident scenario has been presented to illustrate the features of this code version. As a consequence of the containment loads imposed by sodium-concrete and core-concrete interactions in this integral calculation, venting of the outer containment is forced to occur at 20 hours, whereas venting was delayed until 10 days in a previous demonstration calculation for a relatively benign scenario with minimal cavity interactions. While the time to venting is much shorter, the deposition of aerosols is also calculated to occur at much higher rates in the present calculation. As a consequence of the higher deposition rates, the masses of suspended particulate fission products in the outer containment are comparable to or less than those in the previous calculation at the respective times of venting. These high deposition rates are primarily the result of sodium and water condensation on aerosols. These rates clearly could not be properly calculated without the new models available in the LMR/1B-Mod.1 version, including those for the treatment of two condensables, sodium condensation on aerosols, sodium chemistry, hygroscopic aerosols, and concrete

outgassing. The integral demonstration calculation also illustrates the need for mechanistic models of the long-term vaporization release of fission products from pools and of radiative transfer with aerosol scattering. Work in both of these areas has begun at Sandia.

#### REFERENCES

1. K. K. MURATA et al., "User's Manual for CONTAIN 1.1, a Computer Code for Severe Nuclear Accident Containment Analysis," NUREG/CR-5026, SAND87-2309, Sandia National Laboratories, September, 1989.
2. D. E. CARROLL, "Overview of the CONTAIN LMR Code," Sixteenth Water Reactor Safety Information Meeting, Gaithersburg, MD, October 24-27, 1988.
3. A. J. SUO-ANTILLA, "SLAM - A Sodium Limestone Concrete Ablation Model," NUREG/CR-3379, SAND83-7114, Sandia National Laboratories, Albuquerque, NM, December, 1983.
4. F. GELBARD, "Modeling Aerosol Growth by Vapor Condensation," Aerosol Science and Technology, 12, 399 (1990).
5. K. E. WASHINGTON and D. E. CARROLL, "Assessment of Models for Steam Release from Concrete and Implications for Modeling Corium Behavior in Reactor Cavities," SAND88-2329C, Sixteenth Water Reactor Safety Information Meeting, Gaithersburg, MD, October, 1988.
6. R. K. COLE et al., "CORCON-MOD2: A Computer Program for Analysis of Molten-Core/Concrete Interactions," NUREG/CR-3920, SAND84-1246, Sandia National Laboratories, Albuquerque, NM, 1984.
7. D. A. POWERS et al., "VANESA - A Mechanistic Model of Radionuclide Release and Aerosol Generation During Core Debris Interactions with Concrete," NUREG/CR-4308, SAND85-1370, Sandia National Laboratories, Albuquerque, NM, 1986.
8. P. BEIRIGER et al., "SOFIRE-II User Report," AI-AEC-13055, Atomics International, 1973.
9. S. S. TSAI, "The NACOM Code for Analysis of Postulated Sodium Spray Fires in LMRBRs," NUREG/CR-1405, BNL-NUREG-51180, Brookhaven National Laboratory, Upton, NY, March, 1980.
10. F. J. RAHN, "Summary of the LWR Aerosol Containment Experiments (LACE) Program," LACE TR-012, Electric Power Research Institute, January, 1987.
11. D. E. CARROLL et al., "Liquid Metal Reactor Applications of the CONTAIN Code," Presented at the American Nuclear Society Topical Meeting, Seattle, WA, May 1-5, 1988.

TABLE I  
Rate Constants by Release Group for Pool Vaporization Releases

Release Group	Radionuclides	Release Rates ( $s^{-1}$ )
1	Xe,Kr	1.0
2	I	$1.6 \times 10^{-7}$
3	Cs,Rb,Na	$4.8 \times 10^{-6}$
4	Te,Sb	$3.2 \times 10^{-10}$
5	Sr,Ba	$9.6 \times 10^{-10}$
6	Ru,Rh,etc.	$3.2 \times 10^{-10}$
7	La,Ce,Cm,Pu,etc.	$3.2 \times 10^{-10}$

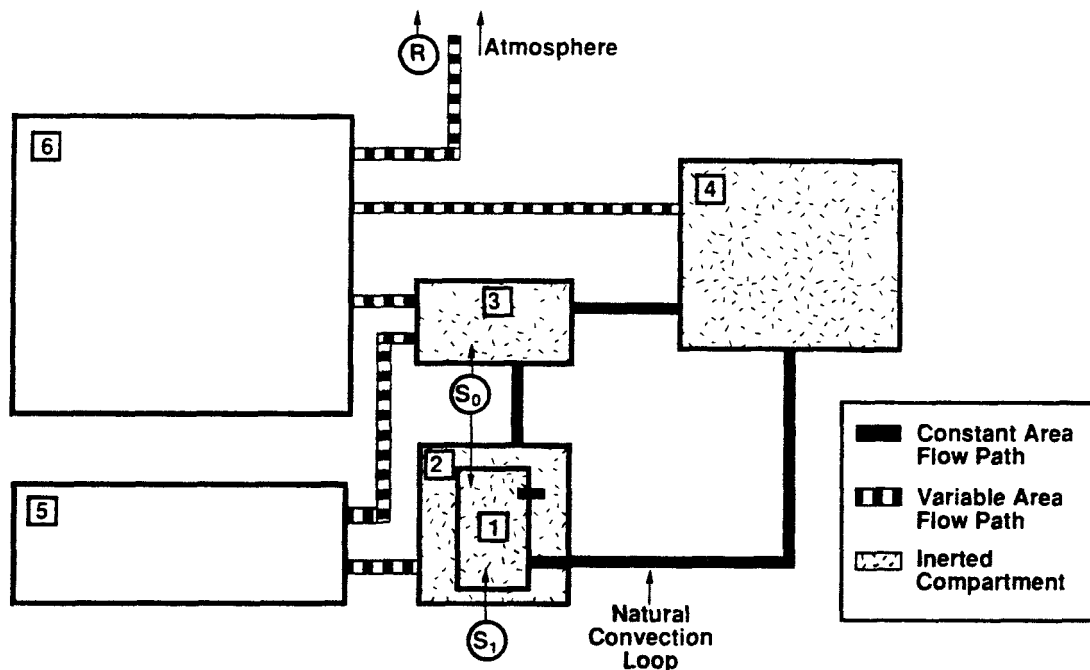


Figure 1. Nodalization of the present integral LMR demonstration calculation (ILMRDC) showing the natural convection loop in the inserted inner containment (cells 1-4), the inserted part of the outer containment (cell 5), and the noninerted part of the outer containment (cell 6). Also shown are the location of the initial radionuclide release from the vessel ( $S_0$ ) at time zero and the location of the pool vaporization release ( $S_1$ ) beginning at vessel melt-through at 3000 seconds.

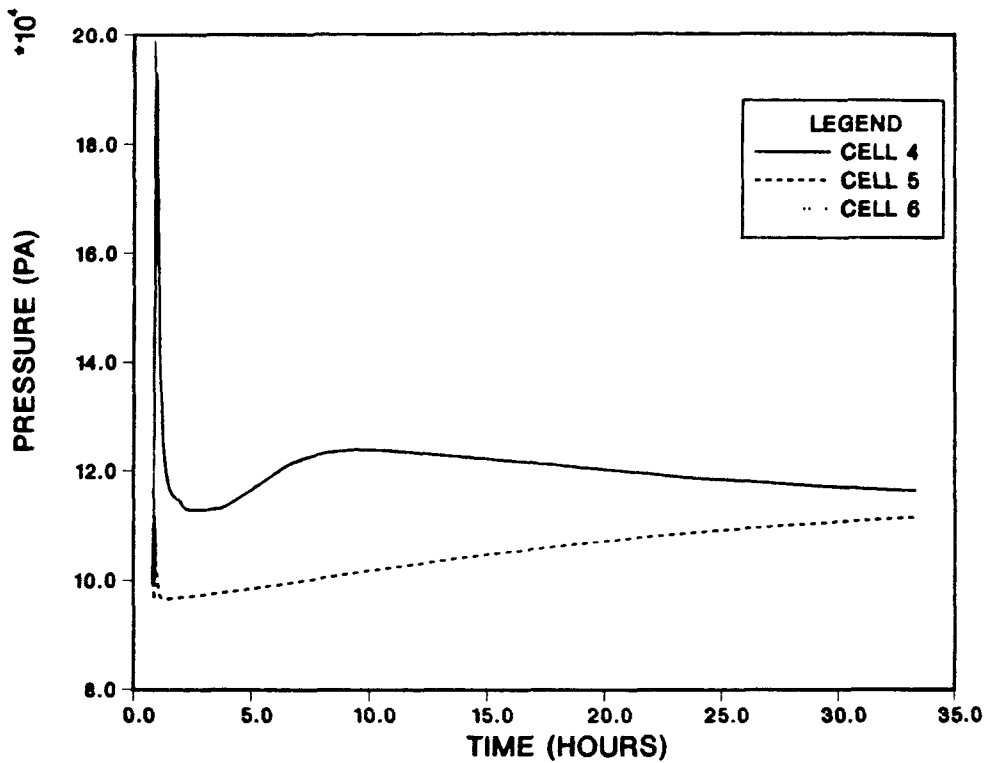


Figure 2. Atmosphere pressures calculated in cells 4, 5, and 6 in the ILMRDC.

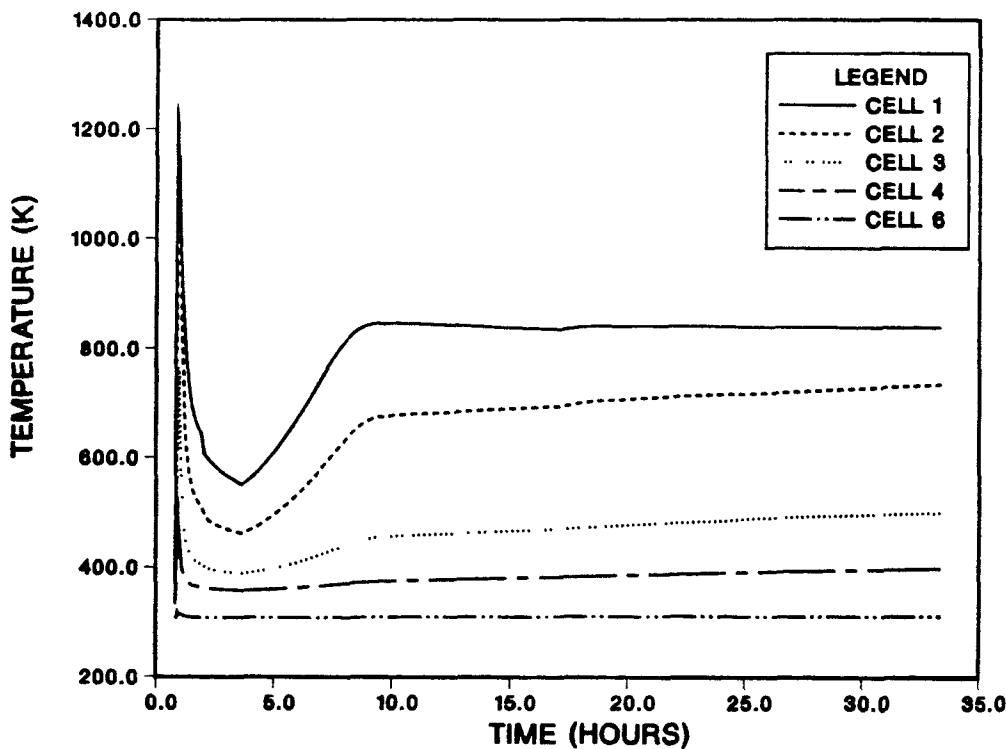


Figure 3. Atmosphere temperatures calculated in cells 1-4 and 6 in the ILMRDC.

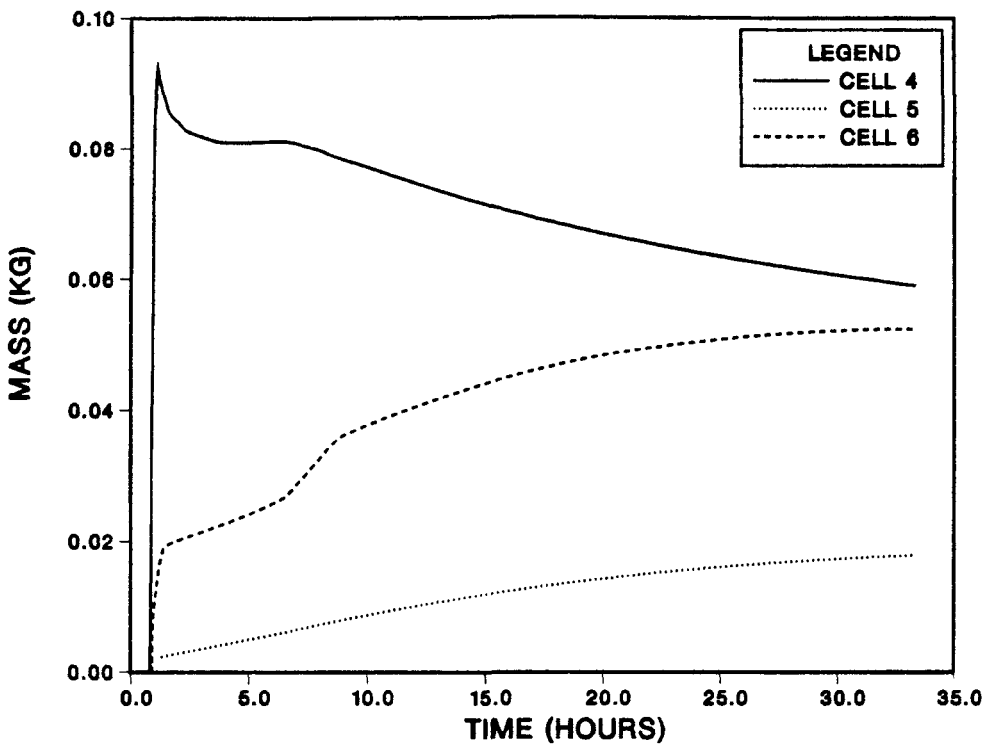


Figure 4. Airborne masses of  $\text{Xe}^{133}$  calculated in cells 4-6 in the ILMRDC.

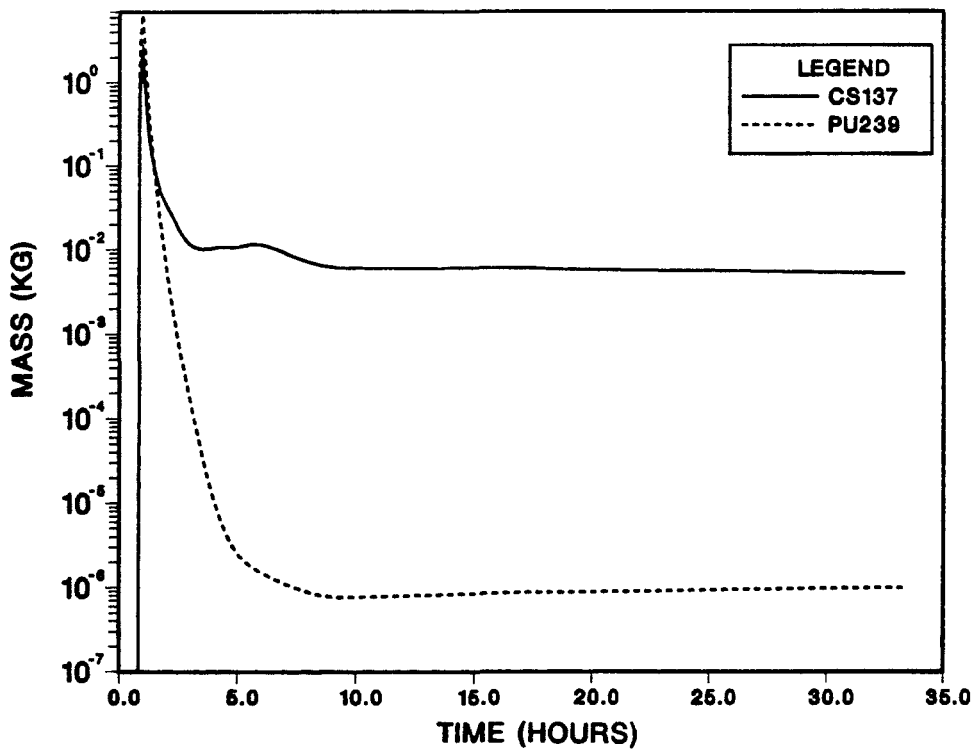


Figure 5. Airborne masses of  $\text{Cs}^{137}$  and  $\text{Pu}^{239}$  calculated in cell 4 of the inner containment in the ILMRDC.

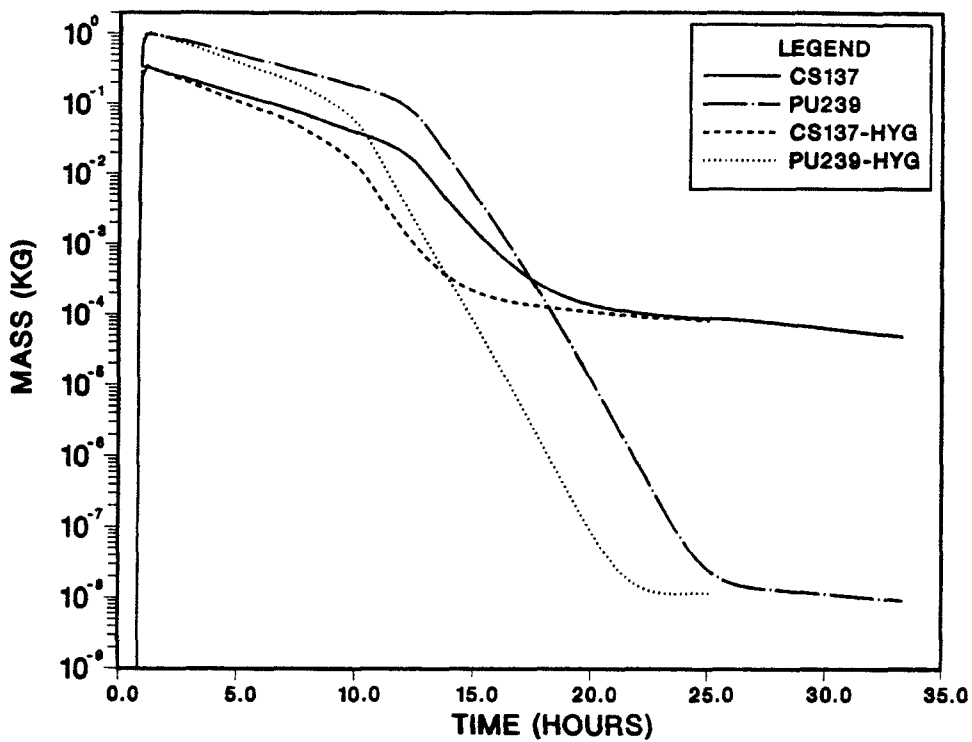


Figure 6. Airborne masses of  $\text{Cs}^{137}$  and  $\text{Pu}^{239}$  calculated in cell 6 of the outer containment in the ILMRDC. The curves for CS137-HYG and PU239-HYG show the effect of modeling the hygroscopic nature of the aerosols present.

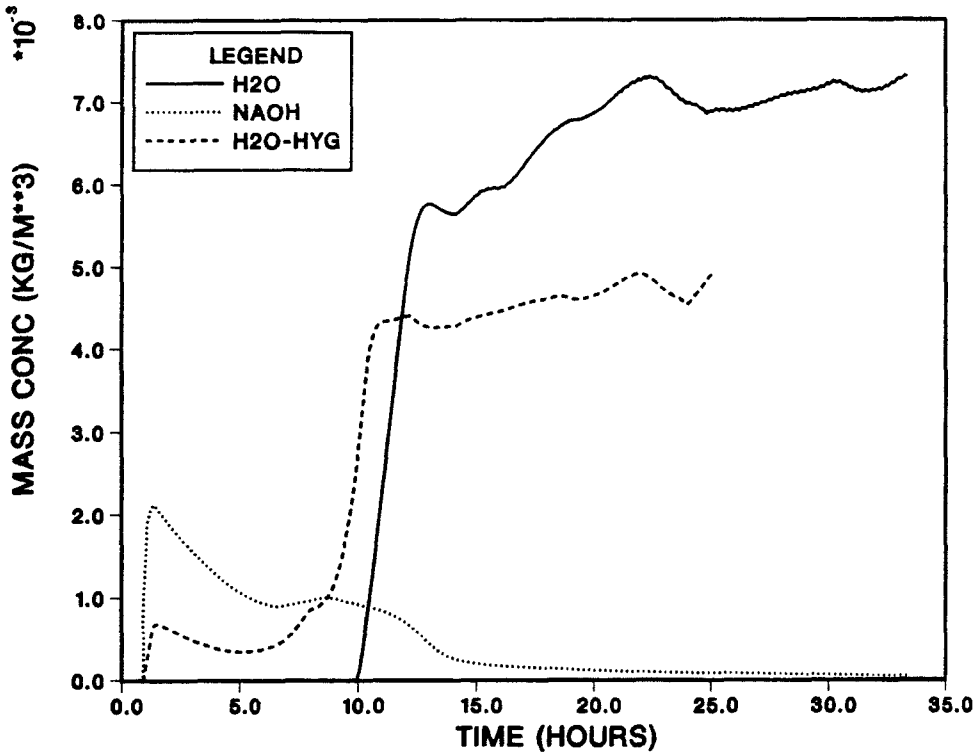


Figure 7. The mass concentrations of water and NaOH aerosols in cell 6 in the ILMRDC without hygroscopic effects; also, the mass concentration of water aerosols when hygroscopic effects are considered (H<sub>2</sub>O-HYG).